Structure of ultrathin films of Mn on Cu(111) investigated by the normal-incidence x-ray standing-wave method

M. T. Butterfield* and M. D. Crapper†
Department of Physics, Loughborough University, Loughborough, LE11 3TU, United Kingdom

V. R. Dhanak
Daresbury Laboratory, Daresbury, Warrington, WA4 4AD, United Kingdom
(Received 15 March 2002; revised 15 July 2002; published 24 October 2002)

The growth of Mn films on Cu(111) has been investigated in the range of 0.5–4.5 monolayer equivalents using the normal-incidence x-ray standing-wave method. The films have been found to be incommensurate at all coverages as determined by the coherent fraction of the Mn in the substrate $(\bar{1}11)$ reflection. The (111) reflection gives a coherent position that increases with coverage, but a coherent fraction that decreases. At submonolayer exposure, the low coherent position reveals that the majority of the Mn atoms are at a *z* position near to, but slightly expanded from, the Cu(111) *d* spacing, but that $15\% \pm 5\%$ of the Mn are at a *z* position of 0.57 ± 0.18 of the substrate *d* spacing. Modeling of the trends in coherent position and fraction with Mn exposure eliminates the possibility of the overlayer being α-Mn, γ-Mn (fcc), or δ-Mn (bcc). However, the trends are entirely consistent with the Mn overlayer being a Laves phase similar in structure to Zn_2Mg.

DOI: 10.1103/PhysRevB.66.165414 PACS number(s): 68.49.Uv, 68.55.−a, 68.55.Ac

I. INTRODUCTION

This paper reports the investigation of the room-temperature growth of Mn overlayers on Cu(111) up to 4.5 monolayer (ML) equivalents using the normal-incidence x-ray standing-wave (NIXSW) method. This is an unusual application of the method, which is particularly sensitive to the formation of well-defined layers in the growing film and to the layer spacings. It has the advantage over many diffraction techniques that it is element specific. Although it is known that at low coverages the Mn alloys with Cu, we show that this does not continue significantly for higher coverages. Modeling of various possible overlayer structures for comparison with the NIXSW data shows that the most probable growth mode is in a Laves phase similar to Zn_2Mg.

The interest in depositing Mn onto Cu surfaces is stimulated both by the possibilities of engineering metastable phases with unusual magnetic properties and because the Mn/Cu system has applications as a catalyst. A recurring theme of Mn adsorption at low coverage is one of the formation of ordered substitutional alloys, despite no ordered three-dimensional alloy being known. The most studied system is that of Mn on Cu(100), which forms a $c(2\times2)$ substitutional alloy at around 0.5 ML coverage.[1] A low-energy electron diffraction (LEED) investigation of Mn on Cu(111) (Ref. 2) reported an incommensurate sixfold symmetric $(\sqrt{3}\times\sqrt{3})R30°$ structure related to α-Mn mixed with small amounts of γ-Mn. The authors of this work related this structure to a similar one reported[3] for the Pd(111) surface at elevated temperatures. The in-plane misfit was $+6.3\% \pm 1\%$ (lattice constant 4.69 Å giving a nearest-neighbor spacing of 2.71 Å), and there was strong evidence of island formation from Auger electron spectroscopy.

A recent scanning tunneling microscopy (STM) investigation of Mn on Cu(111) (Ref. 4) has confirmed the complexity of the submonolayer structure grown at room temperature (320 K). STM images reveal Stransky-Krastanov growth, with a initial flat layer of growth, followed by three-dimensional growth. This growth mode is confirmed by a shoulder in work function measurements at a coverage of about 1 ML. While the more open (100) surface of copper allows incorporation of Mn atoms into the surface, for low coverages on (111) this only happens at steps. Increased deposition forms compact alloy islands of at least two layers of Cu/Mn. This work reported a lattice constant of 4.89 Å (equivalent to a nearest-neighbor spacing of 2.80 Å) and a $(\sqrt{3}\times\sqrt{3})R30°$ superstructure.

There has been little work so far on the extended growth of Mn on Cu(111) beyond the initial alloy formation. In the STM work, three-dimensional deposition was reported to 12 ML, but was not structurally analyzed. However, there are several examples of investigations of the growth of Mn films beyond 1 ML equivalent on other surfaces. A low-energy electron diffraction, Auger electron spectroscopy, and ultraviolet photoemission study of Mn on Pd(111) deposited at room temperature reported[3] that a pseudomorphic three fold (1×1) trigonally distorted fcc epitaxial layer could be prepared with thicknesses up to 20 layers. The in-plane lattice spacing of fcc Mn, 2.73 Å, matches well to the Pd(111) spacing of 2.75 Å. However, the *d* spacing of this structure was smaller than that of Pd(111) by 3.8%. The authors also reported the existence of a $(\sqrt{3}\times\sqrt{3})R30°$ structure that could be prepared at 150 °C. The determination of the structure of this phase proved intractable, but ultraviolet photoemission studies suggested that it was related to α-Mn. In another study, Heinrich *et al.*[5,6] investigated the deposition of Mn onto Ru(0001) using reflection high-energy electron diffraction. The first two layers were found to be pseudomorphic, but beyond this a new (3×1) or $(\sqrt{3}\times\sqrt{3})R30°$ was found. The authors proposed that the Mn on this surface adopted a Laves phase structure related to Zn_2Mg or Cu_2Mg. In this scheme, Mn was effectively forming an intermetallic

compound with itself, the structure having two different Mn sites with different atomic volumes. The rationale behind this idea is that a similar effect is seen in α-Mn and the Laves phase structure has some similarities to α-Mn.

The x-ray standing-wave technique[7,8] is an established method for the determination of the structure of adsorbates on metal and semiconductor surfaces. Under x-ray Bragg reflection conditions the incident and reflected waves interfere to form an x-ray standing wave with a spatial periodicity in intensity equal to that of the atomic planes. As the range of total reflectivity is scanned, the phase of this standing wave moves in space, and the absorption profile of any atom through this range is characteristic of the position of the atom relative to the atomic planes of the substrate. Originally, this experiment was conducted at an arbitrary (often grazing) incidence angle, and the scan was achieved by varying this angle. The ''rocking curve'' so obtained is extremely narrow, limiting applicability to near-perfect crystals. When a Bragg peak is measured by scanning the photon energy at normal incidence to the atomic planes, however, the influence of mosaicity is not a serious problem and typical metal crystals may be used.[8,9] When applied to the (111) reflection of a (111)-oriented crystal, the method provides information about the perpendicular spacing of an adsorbate relative to the spacings of the extended bulk atomic planes. Often a second measurement using the $(\bar{1}11)$ reflection is employed to give a simple geometrical triangulation of the adsorption site.

Recently, it has been shown[10] that, in addition to simple atomic and molecular adsorption systems, NIXSW method may be applied to the more complex systems that are found in metal-on-metal epitaxy. Such systems intrinsically contain several different adsorption sites originating in the different layers of growth, which complicates interpretation of the data. However, the parameters that are usually extracted from an NIXSW analysis—the coherent position and fraction—contain a wealth of information about the layer spacings, the degree of site order, and the incidence of stacking faults, all of which are referenced directly to the substrate and with elemental specificity. We have applied the NIXSW method to the study of the growth of Mn films on Cu(111) for doses equivalent to 0.5–4.5 ML. The aim was to investigate the growth mode of the film beyond the initial stage involving surface alloy formation. Several models of growth have been tested and compared with the observed trends in variation of coherent position and fraction with dosage.

II. EXPERIMENT

The experimental measurements reported in this work were made using station 6.3 (Ref. 11) on the Synchrotron Radiation Source (SRS) at Daresbury Laboratory, UK. Station 6.3 is a dedicated to NIXSW and surface-extended x-ray absorption fine structure (SEXAFS) measurements and is equipped with a double-crystal Ge(111) monochromator capable of delivering x rays in the energy region of the normal-incidence Cu(111) Bragg reflection (2965 eV at room temperature). The system is equipped with a concentric hemispherical electron energy analyzer for electron spectroscopy, which was used both for sample characterization and to monitor the x-ray absorption of surface atoms during the NIXSW measurements. The base pressure remained below 1×10^{-9} mbar throughout the experiment.

A Cu(111) crystal was prepared *ex situ* using the usual methods. *In situ* sample preparation consisted of Ar^+ ion bombardment and annealing to produce a clean and well-ordered surface as judged by x-ray photoelectron electron spectroscopy and low-energy electron diffraction.

Mn was deposited *in situ* from a well-outgassed *K* cell and at room temperature. Dose calibration was made by determining the dose required to form a sharp $c(2\times2)$ low-energy electron diffraction pattern on a separate Cu(100) crystal. This pattern corresponds to 0.5 ML or 0.076 atoms $Å^{-2}$. The source-to-sample distance was the same in each case. On the Cu(111) surface, there are 0.176 Cu atoms $Å^{-2}$. The repeatability of the dosing was assessed using quantitative x-ray photoemission spectroscopy (XPS) measurements.

NIXSW measurements were made of the Mn films using both the normal (111) and 70.2 ° off-normal (111) reflections. The x-ray energy was swept through the Cu(111) Bragg energy, and the absorption of both overlayer and substrate was monitored by determining the intensity of x-ray-induced electron emissions: the $2p_{3/2}$ photoemission in the case of Cu and both the $2p_{3/2}$ photoemission and *LVV* Auger emission for Mn. For each photon energy, the electron emission intensities were determined by recording the difference in number of counts per second on the peak and the background counts off the peak at a slightly higher electron energy.

III. RESULTS

A selection of typical NIXSW profiles is displayed in Fig. 1. These data were collected over a range of Mn doses and for both principal (111)-type reflections of the substrate. In this figure, the abscissa is the photon energy and the ordinate is the difference in counts on and off the $2p_{3/2}$ Mn photoemission peaks.

Quantitative analysis of the NIXSW profiles was carried out using the NIXSWFIT (Ref. 12) routine. This extracts two pieces of information from the profile: the coherent position and the coherent fraction. In the case of a single overlayer site, the coherent position is the *d* spacing of the overlayer relative to the substrate continuation planes in units of the substrate *d* spacing, and the coherent fraction reflects the degree of order. In systems where more than one type of site is occupied, as will be the case here, the picture is not so simple and the values obtained for both parameters will be a function of the values for the individual sites as determined by Eq. (1), where F_c is the coherent fraction, P_c the coherent position, f_j the fractional occupation of the jth site, and z_j is the z coordinate of the jth site. The substrate layer spacing is d. It can be seen that the presence of different sites, perhaps corresponding to different layers of the structure, will reduce the coherent fraction. The degree of reduction in this parameter is sensitive to the z coordinate of each individual site:

$$F_c \exp(2\pi i P_c) = \Sigma f_j \exp(2\pi i z_j/d). \qquad (1)$$

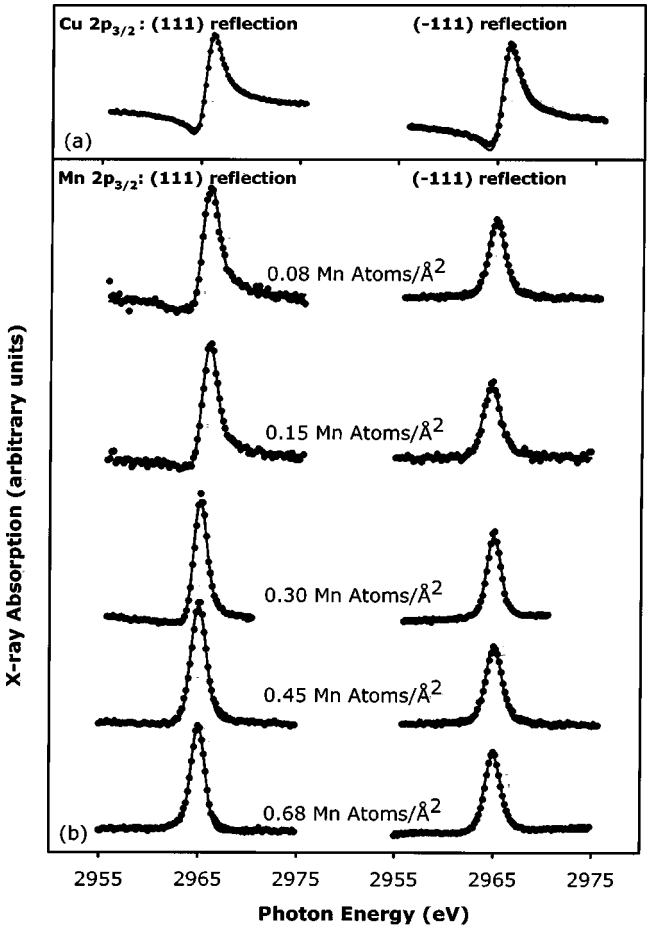

FIG. 1. Typical NIXSW (111) and $(1\bar{1}1)$ profiles (a) for the Cu(111) substrate and (b) for different doses of Mn onto the Cu(111) surface. These data were collected using the Cu $2p_{3/2}$ photoemission and Mn $2p_{3/2}$ photoemission, respectively, to monitor the x-ray absorption. Superimposed on the data is a best fit obtained using the NIXSWFIT routine.

The results of the XSWFIT analysis are shown in Fig. 2. The abscissa in these plots is the Mn dosage, and the ordinate is the value of the parameter. It is usual to quote both of the coherent parameters as a number in the range 0—1, but in this case, we have chosen to express the coherent position in the range 0—2 for the sake of clarity. If P_c is the coherent position expressed in the range 0—1 (where $P_c=1$ is equivalent to $z=d$), then there is no formal distinction between P_c and P_c+n where n is an integer. This is because P_c is simply the value of the position relative to the nearest expected position of the Cu scatterer planes extended out into space above the crystal surface. A similar XSWFIT analysis was carried out for the emission from the Cu substrate. The values for coherent position and fraction were found to be as expected for a Cu(111) surface, indicating no large-scale reconstruction of the surface on the depth scale equivalent to the photoelectron decay length: in this case, around 8 ML. This is a strong indicator that the alloying that is seen at low coverage does not continue for extended coverages. If a large-scale surface alloy was being formed, then the positions of the Cu atoms would be disturbed from their expected bulk positions, modifying the coherent parameters.

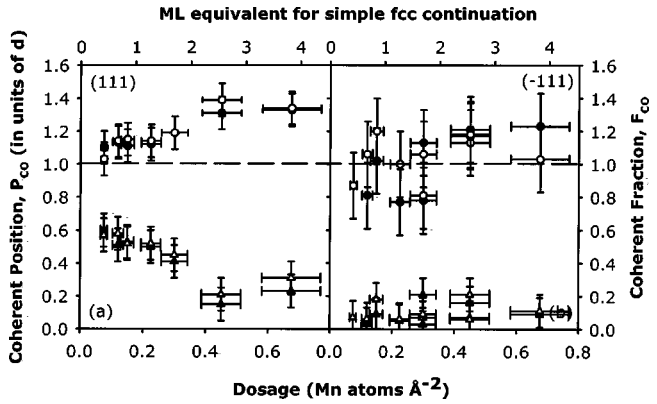

FIG. 2. Plot of the values for the coherent position and coherent fraction of Mn against Mn dosage for (a) the (111) reflection and (b) the $(1\bar{1}1)$ reflection. The coherent positions are denoted by solid circles when determined by $2p_{3/2}$ emission, and open circles when determined by *LVV* emission. The coherent fractions are denoted by solid triangles when determined by $2p_{3/2}$ emission and open triangles when determined by *LVV* emission.

IV. DISCUSSION

Inspection of Fig. 2 immediately reveals several pieces of information about the overlayer system. The first of these is that the coherent fraction for the off-normal $(1\bar{1}1)$ reflection [Fig. 2(b)] is close to zero at all Mn doses. This indicates that the parallel site coherence of the Mn atoms to the substrate is poor, suggesting many different adsorption sites as would occur with either an incommensurate or complex commensurate structure. This is consistent with the findings of other workers[2,4] that the overlayer is incommensurate. The low values of the coherent fractions indicate that the measurements of the $(\bar{1}11)$ coherent position are unreliable and have little meaning.

Turning to the (111) reflection, it can be seen that there are informative trends in both the coherent position and the coherent fraction; the coherent position increases with dosage, whereas the coherent fraction falls. The increasing coherent position can be taken to be a reflection of an overlayer d spacing that is larger than the substrate. So as Mn grows layer on layer, the coherent position of each layer increases incrementally relative to the substrate continuation. If layer-by-layer growth were to occur, then the gradient of the coherent position versus number of layers would be half of the difference between the in-film d spacing and the substrate d spacing, reflecting the fact that all the Mn layers are sampled resulting in a mix of individual site positions. Using such a model, the d spacing of the Mn film would be 14% larger than the Cu(111) d spacing (2.087 Å). However, we must be wary of making such facile interpretations. One problem with this thinking are that the Mn film is known not to grow layer by layer, but instead forms islands, which makes estimating the number of layers difficult. Another problem is that such a model will be invalid if the Mn film adopts a more complicated structure that intrinsically involves more than one d spacing.

The second point to note from Fig. 2(a) is that even at very low dose, the coherent fraction of Mn for the (111)

reflection is much less than that of the substrate (0.59 ± 0.10 compared with 0.84 ± 0.02). While it is known that the growth mode of Mn on Cu(111) involves islanding, so that more than one layer is to be expected, the reduction in coherent fraction cannot be explained simply by the presence of two or three layers that have a d spacing marginally different from the substrate. In fact, the islands would need to be more than five layers thick before such a reduction in coherent fraction could occur. However, the coherent fraction at low dose can be fitted by two layers if the d spacing of one layer is allowed to differ radically from that of the other. The best fit is obtained with $85\% \pm 5\%$ of the atoms at z_1 and $15\% \pm 5\%$ of the atoms at z_2, where $z_1/d = 1.07 \pm 0.04$, $z_2/d = 0.57 \pm 0.18$, and d is the Cu(111) d spacing. That is, a significant proportion of the atoms are at an interlayer spacing near to half that of the substrate. It is known that at low-coverage Mn incorporates into the Cu(111) surface, particularly at steps. However, the NIXSW measurements make it clear that if this incorporation is responsible for the reduction in coherent fraction, then it is not a simple substitution.

The third point to note from Fig. 2(a) is that the (111) coherent fraction decays rapidly with dose revealing an incremental loss of perpendicular site coherence with the substrate. This must originate from an increasing number of sites with dose, relative to the (111) planes of the substrate, resulting primarily from an in-film d spacing that is different from the substrate. The startling feature of this is the rapidity of the fall, which is unlikely to occur in any simple layer-by-layer growth.

A more detailed understanding of the variation in Mn coherent position and fraction with dose can be obtained by testing models of different possible structures against the data. Several models are worthy of consideration. Bulk Mn can have several different structures. At room temperature, it has a complex cubic structure labeled α-Mn, which comprises 29 atoms. This structure is effectively a body-centered-cubic array of hexatetrahedrons containing 12 perimeter atoms and a centering atom. These hexatetrahedrons are linked by two different types of Mn atoms to form the complete structure. Effectively, there are four different types of Mn atoms occupying different atomic volumes. It is difficult to see how this structure could grow epitaxially as it has no densely packed planes suitable for growth: however, it has been included for completeness. Other, higher-temperature phases of Mn include the face-centered-cubic γ-Mn ($1079°C < T < 1143°C$) (Ref. 13) and the body-centered cubic δ-Mn (above 114°C) (Ref. 13). There have been reports that both γ- and δ-Mn can be stabilized at room temperature using epitaxial growth, so these structures are clear candidates for modelling. Additionally, we have modeled the Laves phase Zn_2Mg structure, which has been proposed[5] for Mn overlayers on Ru(0001).

The rationale for testing the Zn_2Mg structure is that, similarly to α-Mn, its basic building blocks are hexatetrahedrons, but comprising Zn edge atoms and a Mg centering atom. Unlike α-Mn, however, the hexatetrahedrons are in a regular array without linking atoms and the structure contains closely packed planes that are suitable for growth. In this model for growth, both Zn and Mg atoms are replaced by Mn atoms, which occupy different atomic volumes. A schematic of the Mn hexatetrahedrons is shown in Fig. 3. The basic building block comprises a hexagonal array of Mn atoms in the first layer, an open triangle of Mn atoms in the second layer, and a solid triangle in the third layer. Inside this hexatetrahedron is an Mn centering atom that is displaced towards the first layer from the second layer by 25%. The hexatetrahedrons are arranged in a hexagonal array within plane, but with alternate ones being inverted providing 50% centering atoms below plane and 50% above. These layers may stack in several ways giving the Zn_2Mg, Cu_2Mg, or Ni_2Mg structures, but the (111) NIXSW reflection would be unable to distinguish these. The attraction of this model for comparing with the NIXSW data is the presence of the centering atoms at very different d spacings, which would result in a large reduction in the coherent fraction of the (111) reflection.

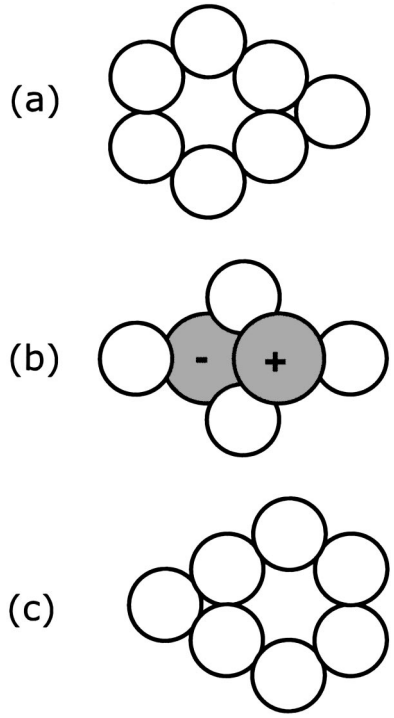

FIG. 3. Schematic diagram of the way in which Mn could adopt the Zn_2Mg Laves phase, showing (a) layer 1 (lower), (b) layer 2, and (c) layer 3 (upper). The open atoms occupy a normal atomic volume and the hatched atoms a larger one. The hatched atoms are displaced from the second-layer z position by $\pm 25\%$.

The models were implemented using a scientific spreadsheet program assuming a Mn-Mn distance of 2.73 Å as is found in bulk Mn.[14] Reasonable adjustments can be made to this distance without changing the conclusions of the work. This distance influences both the interplane distance and the degree of packing within plane in terms of atoms $Å^{-2}$. The z coordinates of the atoms together with their occupation fractions were used to compute the coherent fraction and position that would be measured using the Argand scheme. The computation of the coherent position contains an inherent ambiguity in that the spacing of the Mn-Cu interlayer is not known. Variation of this parameter simply moves the simu-

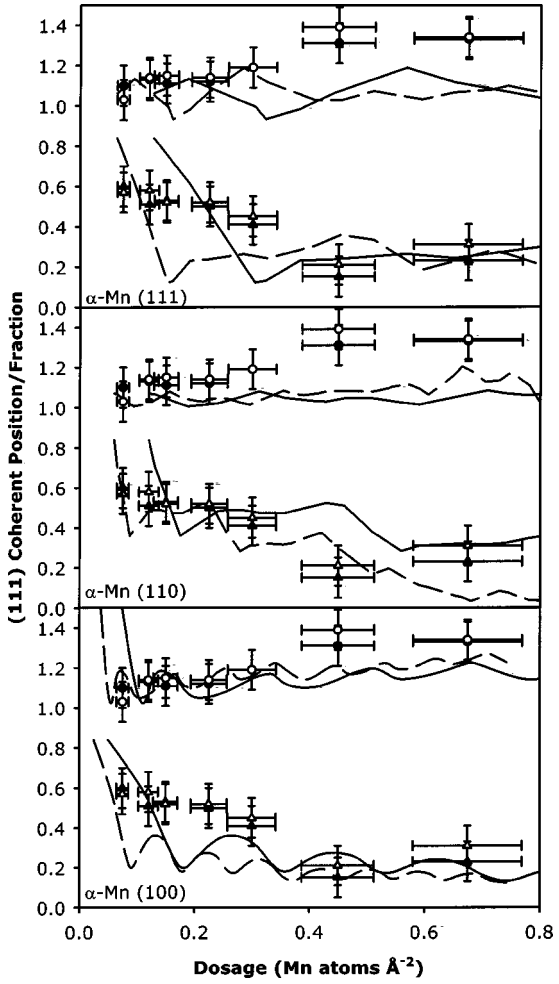

FIG. 4. Plots of the simulated coherent position and fraction for the three low-index orientations of α-Mn. The solid lines represent the behavior for layer-by-layer growth, and the dashed lines are for a structure containing islands. The key for the experimental points is as for Fig. 2.

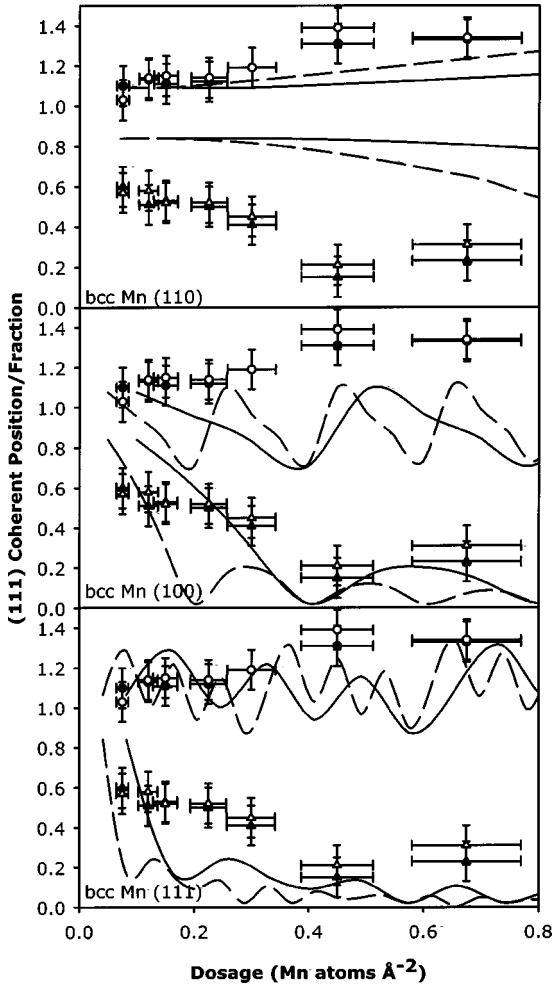

FIG. 5. Plots of the simulated coherent position and fraction for the three low-index orientations of bcc δ-Mn. The solid lines represent the behavior for layer-by-layer growth, and the dashed lines are for a structure containing islands. The key for the experimental points is as for Fig. 2.

lated coherent position curves up and down, so it has been adjusted to fit the data at low coverage. The coherent fraction, however, is intrinsic to the film structure and is not affected by this parameter. It is important to note that owing to the sampling depth of the electrons and penetration depth of the x rays, these parameters are dependent upon the whole depth of the film not simply the surface layer. The effect of islanding was included using a uniform layer occupation of 50%. While crude, the precise details of this assumption have no influence on the conclusion. In fact, owing to the requirement of fitting the variation of both coherent parameters simultaneously, it would appear that this procedure offers a rough method of determining global average layer occupations.

The results of the calculations for the three low index directions of α-Mn are shown in Figs. 4–4(c). The basic calculations for layer-by-layer growth are shown as the solid line, and those with islanding included are shown using a dashed line. The calculations were carried out assuming that the most densely packed plane of the unit cell was the first in the film. It can be seen that these structures do a poor job of simulating the data. A feature of all three orientations is a coherent position that does not increase with dosage; the oscillations induced by the complex structure would average out in any real growth situation. Both the (111) and (110) orientations of α-Mn can be ruled out entirely from the expected behavior of the coherent position. In each case, the calculations underestimate the coherent position and do not reproduce the incremental increase present in the data. Both of these orientations also do a poor, but not totally unacceptable job of simulating the coherent fraction. A little more consideration needs to be given to the (100) orientation. Although it does not do a good job of reproducing the behavior of the coherent position, it cannot be rejected on the basis of this alone. However, the (100) orientation significantly underestimates the values of the coherent fraction for much of the data range. This underestimation is exaggerated when the effect of islanding is included, but the islanding correction is necessary as the presence of Stransky-Krastanov growth is known. It must again be stressed that the growth of Mn films

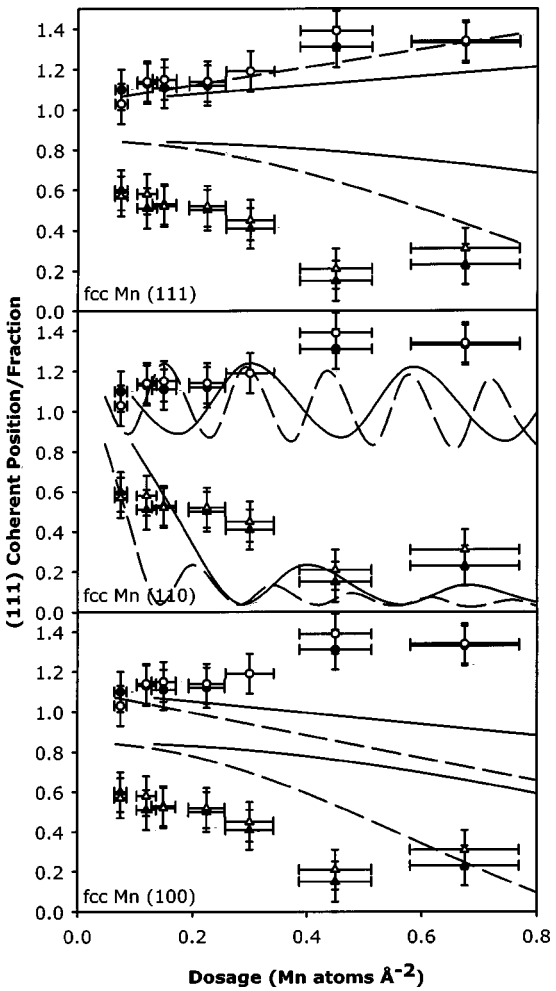

FIG. 6. Plots of the simulated coherent position and fraction for the three low-index orientations of fcc γ-Mn. The solid lines represent the behavior for layer-by-layer growth, and the dashed lines are for a structure containing islands. The key for the experimental points is as for Fig. 2.

with the α-Mn structure is highly unlikely owing to the absence of close-packed planes. For this reason and for the poor job that it does in simulating the data, this model can be rejected.

The results of the simulation for bcc δ-Mn are shown in Fig. 5. A tetragonally distorted form of this structure has been reported to be found in epitaxial growth on some surfaces.[15,16] This structure does a poor job of reproducing the trends in the data. The most likely orientation to be found in growth on an fcc (111) surface is the close-packed (110): however, this can be ruled out by the behavior of the coherent fraction alone. The more open (100) and (111) orientations show features more resembling the data, owing to the more closely spaced planes. However, the (111) orientation can be eliminated as it significantly underestimates the coherent fraction. The (100) orientation is worthy of more consideration. It does not show the general trend in expansion of the coherent position, but the wildly oscillating P_C it predicts passes through many of the data points. The line for the coherent fraction also passes through some of the data

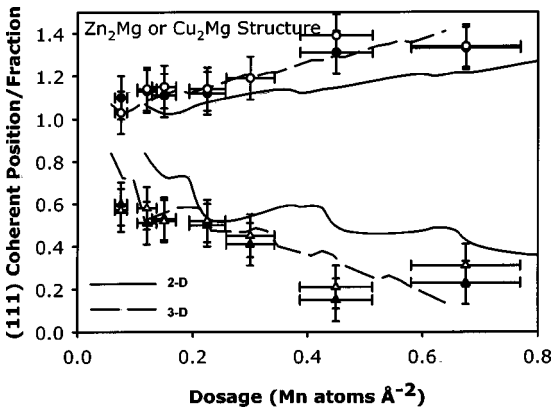

FIG. 7. Plots of the simulated coherent position and fraction for the Zn_2Mg Laves phase. The solid lines represent the behavior for layer-by-layer growth, and the dashed lines are for a structure containing islands. The key for the experimental points is as for Fig. 2.

points. However, when the correction for the islanding is made, the fit to the coherent fraction deteriorates to the point of unacceptability. Studies of the system using STM have shown[4] that the growth is dominated by the formation of islands, so it is necessary to reject this model.

The results of the simulations for fcc γ-Mn are shown in Fig. 6. The (111) orientation might seem most likely to grow on Cu(111) and has been reported in some other growth systems.[3] From the Fig. 6, it can be seen that with the inclusion of the islanding correction this structure can reproduce the incremental increase in coherent position with dosage, but in no way can it be made to reproduce the fall in coherent fraction. The fall in coherent fraction is a strong indicator of a structure that is not a simple layer-by-layer structure such as fcc (111). There are no lattice expansions, either uniform or volume conserving, that can reproduce the behavior observed in the data. The same statements are true of the (100) orientation. Neither does the (110) orientation do a good job of reproducing both trends. On the basis of these simulations, this model must be rejected.

The results of the simulation for the Laves phase Zn_2Mg are shown in Fig. 7. It can be seen immediately that this simulation reproduces the behavior seen in the data very well, particularly when islanding is allowed. The oscillations in the simulation occur as each extra layer is added: the densely packed planes increase the coherent fraction, but the intermediate planes reduce it. In the experimental data, these oscillations will be suppressed by scatter in the number of completed layers. These simulations demonstrate that the growth of Mn on Cu(111) forms a structure related to the Laves phase Zn_2Mg. Precisely which of these related phases is present cannot be determined, and it is possible that a mix exists. The growth of such a phase that does not exist in nature for Mn is perhaps not so surprising, as this structure is related to α-Mn. However, it contains close-packed planes that are more suitable for two-dimensional growth.

The models show some general features that are worthy of discussion. The main point to make is that the models featuring the growth in the densely packed planes of the more common structures show slow variations in the coher-

ent position and fraction and hence cannot be present here. Examples of this are the fcc (111)- and bcc (110)-oriented growth. Both of these produce a coherent fraction that falls slowly, owing to the presence of a single-layer spacing that is similar to the Cu(111) substrate. The only structure featuring a densely packed growth plane to reproduce the behavior in coherent fraction is the Laves structure. This is due to the presence of three different interlayer spacings. The fall in coherent fraction can be mimicked by some of the more open and less probable structures simply by having an interlayer spacing very different from the substrate. However, these open structures in general do not mimic the behavior of the coherent position. The behavior of the coherent position with dosage indicates that the average *d* spacing of the film is similar to that of the substrate, but the rapid fall in coherent fraction is not consistent with growth within layers having uniform separation. The simulations for α-Mn show some features that resemble the data, and this is not surprising since α-Mn is based on similar hexatetrahedrons. However, the simulations for this structure all have a much poorer fit to the data than that of the Laves phase, and it is difficult to envisage how such a complex structure could grow in a two-dimensional epitaxial film. Hence the only model that satisfies all requirements is the Laves phase, typified by Zn_2Mg.

V. CONCLUSION

NIXSW measurements of ultrathin films of Mn on Cu(111) using the $(\bar{1}\bar{1}1)$ reflection have shown that the films are incommensurate. The (111) reflection shows that the films have a *d* spacing slightly larger than the Cu(111) *d* spacing, but that the films rapidly become incoherent with the substrate.

Quantitative modeling of the data has shown that they are indicative of an epitaxial structure that involves Mn atoms with several different *d* spacings relative to the Cu(111) *d* spacing. The models have shown that the data are consistent with the existence of a Laves phase related to Zn_2Mg. In this structure, originally proposed by Heinrich *et al.*, there are two different types of Mn with different atomic volumes.

We have shown that NIXSW is an effective method for the investigation of metal-on-metal epitaxy. The evolution of the coherent fraction with dosage is a sensitive measure of the number and nature of the perpendicular sites that are present—effectively to the number and nature of the atomic planes.

ACKNOWLEDGMENT

This work was supported by the EPSRC via the provision of access to the SRS and support for M.T.B. George Miller provided technical support at the SRS.

Present address: Condensed Matter and Thermal Physics Group MST-10, Mailstop K764, LANL, Los Alamos, NM 87545.
†Author to whom correspondence should be addressed.

[1] D. Brown, T. C. Q. Noakes, D. P. Woodruff, P. Bailey, and Y. Le Goaziou, J. Phys.: Condens. Matter **11**, 1889 (1999).
[2] D. Tian D, A. M. Begley, and F. Jona, Surf. Sci. Lett. **273**, L393 (1992).
[3] D. Tian, H. Li, S. C. Wu, F. Jona, and P. M. Marcus, Phys. Rev. B **45**, 3749 (1992).
[4] J. Schneider, A. Rosenhahn, and K. Wandelt, Appl. Surf. Sci. **142**, 68 (1999).
[5] B. Heinrich, A. S. Arrott, C. Liu, and S. T. Purcell, J. Vac. Sci. Technol. A **5**, 1935 (1986).
[6] B. Heinrich, C. Liu, and A. S. Arrott, J. Vac. Sci. Technol. B **3**, 766 (1984).
[7] J. Zegenhagen, Surf. Sci. Rep. **18**, 199 (1993).
[8] D. P. Woodruff, Prog. Surf. Sci. **57**, 1 (1998).
[9] D. P. Woodruff, D. L. Seymour, C. F. McConville, C. E. Riley, M. D. Crapper, and N. P. Prince, Surf. Sci. **195**, 237 (1988).
[10] M. T. Butterfield, M. D. Crapper, T. C. Q. Noakes, P. Bailey, G. J. Jackson, and D. P. Woodruff, Phys. Rev. B **62**, 16 984 (2000).
[11] A. A. McDowell, D. Norman, J. B. West, J. C. Campuzano, and R. G. Jones, Nucl. Instrum. Methods Phys. Res. A **246**, 131 (1986).
[12] R. G. Jones (unpublished).
[13] *CRC Handbook of Chemistry and Physics*, 75th ed., edited by D. R. Lide (CRC, Boston Ronge, 1994).
[14] http://www.webelements.com
[15] Y. Tian and F. Jona, J. Phys.: Condens. Matter **13**, 1805 (2001).
[16] S. Andrieu, M. Finazzi, Ph. Bauer, H. Fischer, P. Lefevre, A. Traverse, K. Hricovini, G. Krill, and M. Piecuch, Phys. Rev. B **57**, 1985 (1998).